

Experiment Report Form



Experiment title: Understanding TRIP by linking grain- and sample-scales in 4D		Experiment number: MA 4974
Beamline: ID11	Date of experiment: from: 1. Feb. 2022 to: 8. Feb. 2022	Date of report: <i>Received at ESRF:</i>
Shifts: 21	Local contact(s): Dr. Eleanor Lawrence Bright	
Names and affiliations of applicants (* indicates experimentalists): Dr. BOENISCH Matthias*, KU Leuven Dr. BRODU Etienne*, KU Leuven Mr. DHEKNE Pushkar*, KU Leuven Prof. Dr. PANTLEON Wolfgang, Technical University of Denmark Prof. Dr. SEEFELDT Marc*, KU Leuven		

Report: Metastable austenitic stainless steels (MASS) - a class of transformation-induced plasticity (TRIP) alloys with widespread use in transportation, healthcare and chemical industries - deform by a combination of martensitic transformation and slip, enabling superior strain-hardening and ductility. During straining, a dynamically changing microstructure of grains composed of austenite and martensite forms, governing the macroscopic mechanical performance. Detailed insight into the grain-level mechanics is crucial to improve formability, fatigue resistance and strength, as well as to develop precise material models for computer simulations of industrial forming processes.

For this purpose, we performed combined diffraction contrast tomography (DCT) and in-situ scanning 3D X-ray diffraction (3DXRD) experiments at ID11 on an EN 1.4310 MASS with an austenite grain size of ~100 μm, aiming to reveal the interdependence of TRIP and the 3D microstructure in a phase-, grain-, and time-resolved manner.

Dog-bone shaped tension samples with a square cross-section of 0.8·0.8 mm² (Fig. 1a) were prepared from annealed, strain-free 1.5 mm thick sheets by electrical discharge machining (EDM). At the beamline, austenite

(a) 	(b)									
	DCT/scanning 3DXRD characteristics									
Sample	Strain (%)	Method	Horizontal beam size (μm)	Vertical beam size (μm)	Horizontal step size (μm)	Horizontal steps	Vertical step size (μm)	Vertical steps	Rotation range (°)	Duration vertical step (h)
1	0	DCT	~1000	500						~2.5
	0, 1, 3, 5, 10	3DXRD	2.3	1.6	2.5	120	20	7	210	~9.5
2	0	DCT	~1000	200			200	4		~2.5
	0, 5, 10	3DXRD	2.3	1.6	2.5	160	20	7	260	~16

Figure 1: (a) Tension specimen. (b) Overview of X-ray microscopy methods employed at each applied strain and the corresponding most relevant scan characteristics.

grain size and phase volume fractions were validated by near-field diffraction contrast projections and far-field powder diffraction patterns, respectively. Based on these preliminary measurements, two samples were chosen for in-situ tension combined with scanning 3DXRD. For tensile loading the Admet load rig equipped with a 500 N load cell available at ESRF was used. Prior to mounting the load rig, DCT datasets of the central gauge sections of both undeformed samples were recorded. DCT and in-situ 3DXRD setups are illustrated in Fig. 2. Figure 3a shows a horizontal slice of a reconstructed DCT scan for sample 1. An overview of the methods (DCT, scanning 3DXRD) applied at each tensile strain level together with the method parameters is given in Fig. 1b. All experiments were carried out at a photon energy of 65.35 keV. While for DCT a broad beam, covering the sample cross-section and 200-500 μm high, was used, the beam was focussed down to $2.3 \cdot 1.6 \mu\text{m}^2$ (horizontal·vertical) using Kirkpatrick-Baez mirrors for scanning 3DXRD.

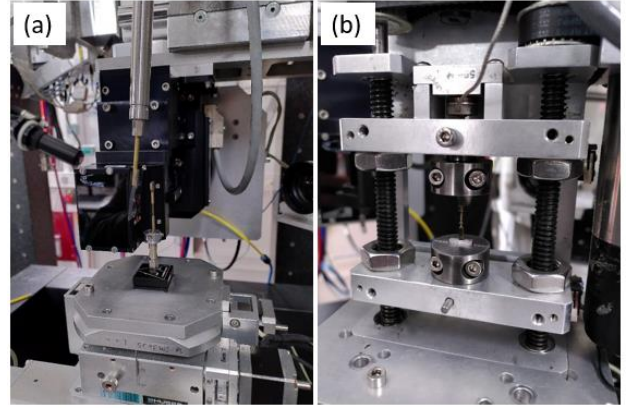


Figure 2: (a) DCT setup for sample to detector distance of $\sim 10\text{mm}$ and detector pixel size of $3.1 \cdot 3.1 \mu\text{m}^2$. (b) Admet stress rig with stainless steel sample inserted used for in-situ scanning 3DXRD (sample to detector distance $\sim 17\text{cm}$ at a detector pixel size of $14 \cdot 14 \mu\text{m}^2$).

Sample 1 was deformed in four increments to 10% tensile strain (Fig. 1b). At each strain increment including the undeformed state, 7 scanning 3DXRD datasets were acquired in $20\mu\text{m}$ steps along the gauge section. At each increment a region of $300 \mu\text{m} \cdot 120 \mu\text{m}$ (horizontal · vertical) was thus covered. On-site analysis showed that only few grains remained in the scanned volume for all rotation angles. Thus for sample 2, the scan width was increased to $400 \mu\text{m}$ and the rotation range increased to 260° to capture more Friedel pairs. Due to the longer scan durations, two increments up to 10% total strain were performed. Data analysis is ongoing. The simultaneous activity of plasticity and martensitic phase transformation seriously complicate the 3DXRD reconstruction schemes. Currently, approaches are being tested to reliably identify peak positions from background-segmented images in a semi-automatic way, despite (i) peak overlap due to presence of austenite and martensites, (ii) peak smearing/broadening due to plasticity and (iii) various noise sources (Fig. 3b, c).

In addition, we carried out a continuous loading in-situ tension test up to fracture to measure the global evolution of austenite and martensite phase fractions during tension. Far-field diffraction patterns were recorded continuously as the sample was rotated back and forth during tensile straining.

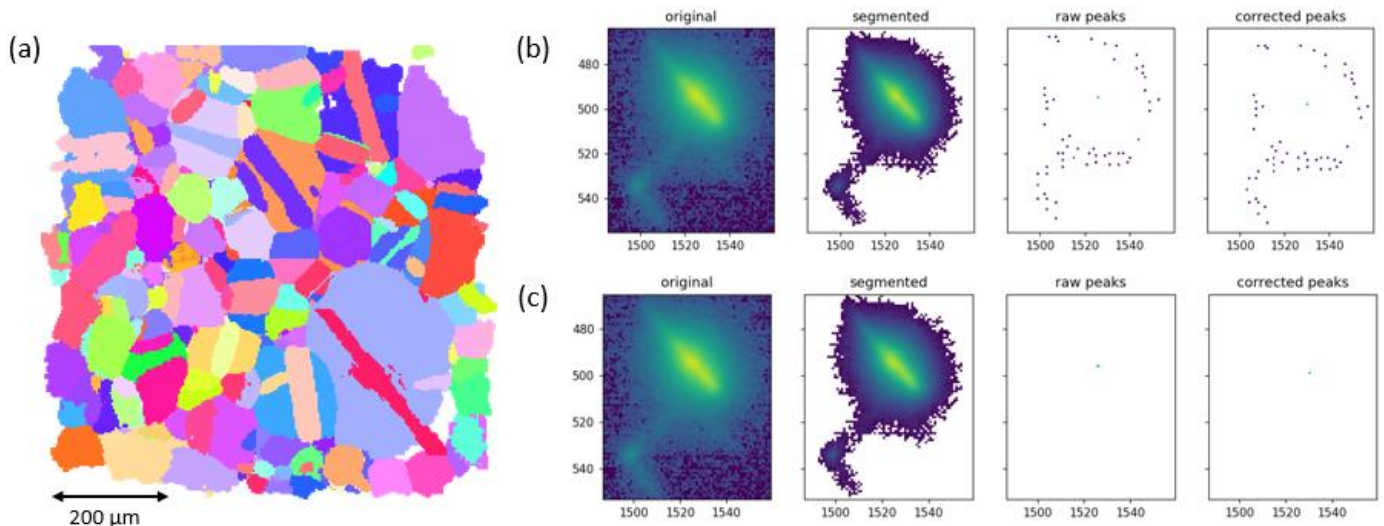


Figure 3: (a) A horizontal slice (perpendicular to sample axis) of a DCT reconstruction of the annealed, undeformed state. (b,c) Connected and smeared out diffraction spots after 5% plastic strain. Peak locations extracted from a segmented image by searching for (b) local maxima and (c) by global maxima, including spatial distortion correction.

Acknowledgements: M. Boenisch acknowledges funding through a Senior Postdoctoral Fellowship by Research Foundation - Flanders (FWO).